

Magnetization Transfer Mapping of Myelinated Fiber Tracts in Living Mice at 9.4 T

S. Boretius¹, P. Dechent², J. Frahm¹, and G. Helms²

¹Biomedizinische NMR Forschungs GmbH, Max-Planck-Institut für biophysikalische Chemie, Göttingen, Germany, ²MR-Research in Neurology and Psychiatry, University Medical Center, Göttingen, Germany

Introduction

MRI of mouse models emerges as an integral part of translational research on white matter (WM) diseases and myelin disorders. Other than in humans, the WM tracts in mouse brain are tenuous structures and exhibit a reduced contrast to adjacent gray matter (GM). Delineation of a specific myelinated tract with sufficiently high contrast is an ongoing endeavor. Next to diffusion tensor imaging (1), magnetization transfer (MT) MRI is known to have a high sensitivity for myelination (2). Recently, a novel FLASH-based MT parameter has been established for neuroimaging of humans (3), which enhances the contrast between GM and WM (4) and, for example, delineates the WM tracts within the thalamus (5). The aim of this study was to evaluate the potential of this approach for the detection of WM tracts in the mouse brain *in vivo*.

Methods

Adult NMRI mice were anesthetized by 1-1.5% isoflurane in a mixture of oxygen and ambient air. They were positive ventilated via an endotracheal tube. 3D FLASH MRI (TR/TE = 14.9/3.9 ms, 1 hour measuring time) was performed at 9.4 T (Bruker Biospin) with 100 μ m isotropic spatial resolution using a 4-element phased-array surface coil (Bruker Biospin) for signal reception. Three different contrasts were acquired: a T1-weighted dataset (flip angle 12°) and two proton density datasets (flip angle 5°), one without and one with MT-weighting by Gaussian-shaped off-resonance irradiation (frequency offset 3kHz, pulse duration 3.5 ms, flip angle 135°). The latter two yielded maps of the MT ratio. The MT saturation (MTsat), that is the percentage of magnetization destroyed by a single MT pulse, was calculated from the MT-weighted signal by correcting for the signal amplitude and T1 (derived from the first two scans) as detailed in (3). A mild Gaussian filter ($\sigma = 1$ pixel, 3x3 kernel) was applied for noise reduction prior to the calculations.

Results

The MTsat map showed a better GM-WM contrast than the MTR and T1 maps (Figure 1). Unlike the original MT-weighted (MTC) images, it does not suffer from surface coil-related signal inhomogeneities as seen in cerebellum and cortex. Typical MT values were 1.1 ± 0.1 % in hippocampus and 2.2 ± 0.2 % in corpus callosum (cc). In addition to large WM tracts such as the cc and internal capsule (int) even smaller structures such as the mammillothalamic tract (mtt) and the fasciculus retroflexus (fr) could be clearly delineated (Figure 2).

Discussion

The MTsat maps were able to distinctly highlight WM tracts even in the small and less myelinated mouse brain – in comparison to humans. This is due to the inherent correction for T1 (3), which in MTC images and MTR maps reduces the GM-WM contrast (6). MT is correlated to the amount of structural material, especially myelin (7). Also GM structures such as the striatum are likely to reflect the content of myelinated axons. MTsat maps may become of great value for the characterization of mouse models of neurodegenerative diseases. The lower MT values in GM and WM compared to human applications mainly reflect the reduced power and larger offset of the MT pulses. Thus, the optimization of sequence parameters (5) may further improve the image quality.

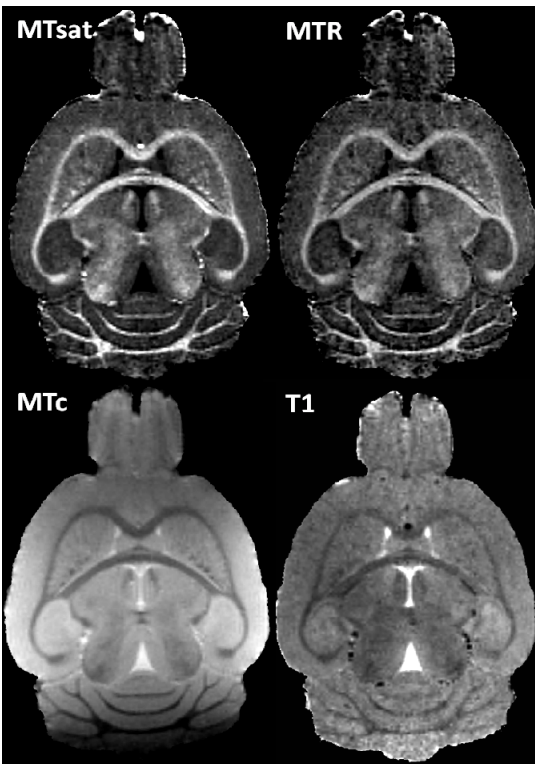


Fig. 1: Horizontal MT-based images and T1 map of a mouse brain *in vivo*.

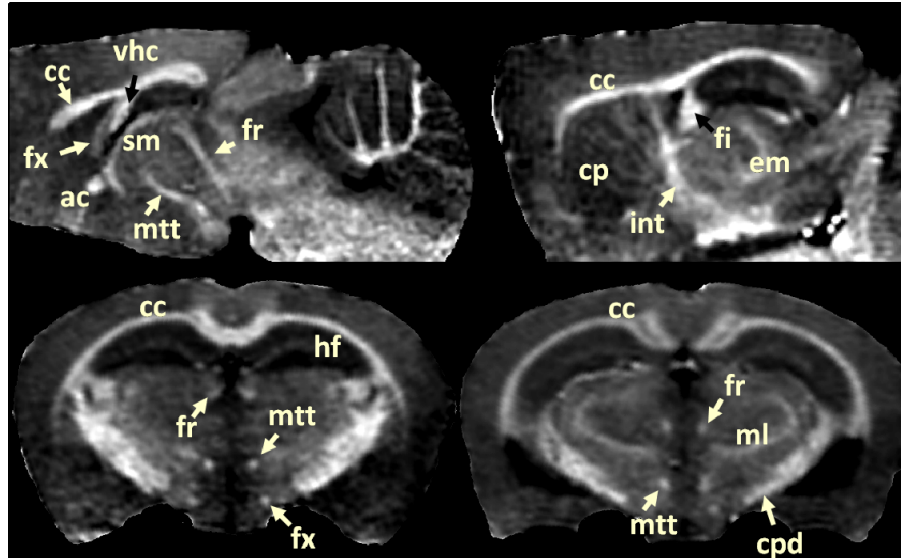


Fig 2: Sagittal (top) and axial (bottom) MT saturation maps of a mouse brain *in vivo*. ac = anterior commissure, cc = corpus callosum, cp = caudate putamen, cpd = cerebral peduncle, em = external medullary lamina of thalamus, int = internal capsule, ml = medial lemniscus; fi = fimbria, fr = fasciculus retroflexus, fx = fornix, hf = hippocampal fissure; mtt = mammillothalamic tract; sm = stria medularis, vhc = ventral hippocampal commissure.

References:

- [1] Boretius et al, *NeuroImage* 47:1252 (2009);
- [2] Natt et al, *MRI* 10:1113 (2003);
- [3] Helms et al, *MRM* 60:1396 (2008);
- [4] Helms et al, *NeuroImage* 47:194 (2009);
- [5] Gringel et al, *JMRI* 29:1285, (2009);
- [6] Helms et al, *Proc ISMRM* 17 (2009);
- [7] Stanisz et al, *MRM* 42:1061 (1999)